Langmuir

ARTICLE

pubs.acs.org/Langmuir

Pore-Spanning Lipid Membrane under Indentation by a Probe Tip: A Molecular Dynamics Simulation Study

Chen-Hsi Huang,[†] Pai-Yi Hsiao,[*,†] Fan-Gang Tseng,[†] Shih-Kang Fan,[∥] Chien-Chung Fu,[‡] and Rong-Long Pan[§]

[†]Department of Engineering and System Science, [‡]Institute of NanoEngineering and MicroSystems, and [§]Department of Life Sciences, National Tsing Hua University, Taiwan, Republic of China

[∥]Department of Materials Science and Engineering, National Chiao Tung University, Taiwan, Republic of China

ABSTRACT: We study the indentation of a free-standing lipid membrane suspended over a nanopore on a hydrophobic substrate by means of molecular dynamics simulations. We find that in the course of indentation the membrane bends at the point of contact and the fringes of the membrane glide downward intermittently along the pore edges and stop gliding when the fringes reach the edge bottoms. The bending continues afterward, and the large strain eventually induces a phase transition in the membrane, transformed from a bilayered structure to an interdigitated structure. The membrane is finally ruptured when the indentation goes deep enough. Several local physical quantities in the pore regions are calculated, which include the tilt angle of lipid molecules, the nematic order, the included angle, and the distance between neighboring lipids. The variations of these quantities reveal many detailed, not-yet-specified local structural transitions of lipid molecules under indentation. The force−indentation curve is also studied and discussed. The results make a connection between the microscopic structure and the macroscopic properties and provide deep insight into the understanding of the stability of a lipid membrane spanning over nanopore.

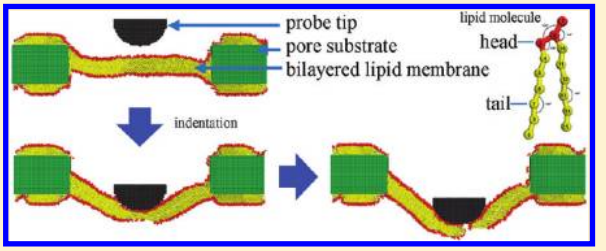

I. INTRODUCTION

Lipid molecules are one of the fundamental components in cells. They can aggregate and form cell membranes, which are a prototype of self-assembly systems found in nature.[1,2] A lipid molecule is generally composed of a hydrophilic headgroup and one or two hydrophobic tails. The assembly of lipid molecules into a two-layered planar structure, with the lipid tails pointing inward toward the bilayer and the headgroups pointing outward in contact with the watery environment, forms an impenetrable barrier to ions and molecules to maintain unique chemical and physiological environments from the two sides of the bilayer.

During the past few decades, the characteristics of lipid bilayers have been widely studied, such as the features of different phases,[3−6] membrane fusion,[7−9] and phase transitions.[10−14] Temperature usually has a strong effect on the arrangement of lipid molecules and the structure of lipid bilayers. (See, for example, ref 15 for an experimental review and ref 16 for a simulation study.) At high temperature, lipid molecules form a liquid-crystalline phase L_α with the tails of the molecule distributing inside the membrane in a disorderly way. This phase is characterized by a small membrane thickness, a large surface area per lipid, and a high lipid molecule mobility. At low temperature, lipid molecules exhibit a gel phase L_β, which is a two-layered structure. Depending on the chemical structure of lipids, the gel phase can be categorized to be nontilted or tilted. In a nontilted gel phase, the tails of the lipid molecules are perpendicular to the surface of the bilayer whereas the tails in a tilted gel phase are oblique. Moreover, for some lipid molecules, the interdigitation of a gel phase is observed. The interdigitated gel phase, denoted by $L_{\beta I}$, is a phase in which the tails of the lipid molecules in the two leaflets of the bilayer interpenetrate, resulting in an extension of the lateral dimension of the membrane.[12] This phase is distinguished by a small membrane thickness, a very large area per lipid, and high ordering.

Recently, lipid membranes have been integrated into the applications of microelectro-mechanical systems (MEMS).[17−22] Because lipid molecules are the basic materials of cell membranes, they are ideal for serving as a platform in biological research to investigate, for example, the functions of membrane proteins. Conventionally, a lipid membrane in the study is spread over the surface of a planar substrate. It is called a solid-supported lipid membrane.[23−28] Solid-supported lipid membranes are very stable and homogeneous.[29] However, the presence of the supporting substrate introduces an additional surface effect into the system and the compartment space below the membrane does not exist anymore. Hence, it restricts the possibility to investigate the properties of lipid membranes under many physiological conditions such as the functions of membrane proteins in the transportation of matter, the mechanism of ion flux through a membrane, and so on.[30]

Received: May 27, 2011
Revised: August 4, 2011
Published: August 22, 2011

To overcome these problems, free-standing membranes have been proposed in some applications.[31−33] In this method, lipid membranes are suspended over pores and hence the space is divided into upper and lower compartments, similar to the one divided by a real cell membrane. It provides a controllable platform for investigating membrane proteins under circumstances close to their native environments, without the superfluous surface effect coming from the solid-supported substrate.

Since 2000, different kinds of free-standing lipid membrane systems have been developed for a variety of studies. Hennesthal and Steinem have applied scanning force microscopy to study the structure of lipid membranes supported by a porous hydrophilic alumina substrate.[31] In their study, the pores were nonpierced cavities on an alumina substrate so that lipid membranes suspended on such pores can be investigated only from the top side. Because the substrate is hydrophilic, the free-standing membranes were entirely supported above the pores instead of spanning over them, which made the applications more restricted in comparison with pore-spanning cases.[34]

The pore-spanning lipid membranes are formed on open hydrophobic pores. Recently, researchers have used them to study embedded membrane proteins. For example, Simon et al. have fabricated arrays of pores on a synthetic silicon layer and formed a biomimetic lipid membrane spanning over the pores for the study of indentation by atomic force microscopy (AFM).[20] They found that the lipid membranes on small pores are more stable over time than on large pores. Moreover, under mechanical stress, the lipid membranes retain an elastic behavior when suspended on small pores, whereas they are irreversibly deformed when suspended on large pores. Gonçalves et al. have reported a 10% area expansion of lipid membranes spanning a 150-nm-diameter pore and a 3 nN yield force when rupture occurs by AFM indentation.[35] They discussed how to use this two-compartment membrane system to study the conformational changes in membrane proteins drawn by gradients, cargo transports, and external forces.

Although the free-standing lipid systems have shown great promise in biological research, there are still many difficulties in maintaining the stability of such systems: the suspended lipid membrane is easily broken by the action of an external force or by small environmental perturbations such as temperature fluctuations, substrate vibrations, and so on. Therefore, one crucial problem in applying the platform systems successfully is to increase the stability of the membrane system. To achieve this goal, a thorough knowledge on the mechanical properties of a lipid membrane under bending and stretching is necessary, especially on the molecular scale.

A series of early experiments regarding the mechanical properties of lipid membranes have been conducted since 1981.[36−41] Evans et al. used a micropipet to study the mechanical properties of a giant vesicle under tension. They found that an abrupt rupture happens when the tension reaches a critical value, and the critical value increases significantly when the loading rate of the tension is high.[37,41] Following the experimental studies, simulations have also been performed to study these topics.[42−44] Neder et al. have employed Monte Carlo simulations to study the conformational transitions of lipid membranes under surface tension at various temperatures in bulk solutions.[44] They found that tension can induce the interdigitation of a lipid bilayer. This discovery is important in understanding the microscopic properties of lipid membranes, which are generally hard to obtain from experiments. Moreover, the mechanical properties of lipid membrane have also been studied by probe indentation. Steinem et al. have systematically studied the indentation of lipid membranes suspended on pores under various conditions by changing the type of lipid molecules, pore size, AFM tips, and so on.[31,34,45,46] They found that the force−indentation curve is governed by the lateral tension (called the prestress effect) when a membrane is suspended on a hydrophobic substrate, which leads to linear behavior. However, the force−indentation curve is dominated by bending and stretching stresses when it is suspended on a hydrophilic substrate, which may contribute to nonlinear behavior.

Despite many efforts, the mechanism that causes the rupture of a suspended lipid membrane under tension is still not clear at the current stage. The lack of information about the internal structure of the membrane systems leads to many open questions. For example, how does the rim of a nanopore interact with lipid molecules when the membrane spans it? Does the internal structure of the membrane, in addition to the external structure, change with indentation by an AFM tip? Insight from a molecular perspective is important in revealing the mechanism and answering these questions.

In this study, we employ nonequilibrium molecular dynamics (MD) simulation to investigate the phenomena of lipid membranes under indentation. The research topics include both the transition of the local arrangement of lipid molecules and the study of the membrane morphology. Several structural and mechanical properties are studied. Recently, Chandross et al. have performed molecular dynamics simulations to study the nanotribological properties of a self-assembled monolayer (SAMs) on amorphous silica during an indentation process.[47,48] They investigated the dependence of the normal and friction forces on several factors, including the tip size, chain length, and binding interaction. Wallace and Sansom have performed steered MD simulations to study a block of carbon nanotubes (CNTs) penetrating a lipid bilayer in bulk solutions.[49] Their study provided useful information concerning the insertion of a hard tubule through a lipid membrane. However, in their work, the effect due to the supporting substrates and the possible rupture mechanism are not discussed. To the best of our knowledge, this is the first time that the mechanical properties of a lipid membrane suspended on a nanopore have been studied by simulations and tested by an indenting probe.

The remainder of the article is organized as follow. In section II, the simulation model and setup are described. The results are presented and discussed in section III. We first present test runs to verify the validity of the setting of our simulation model (in section III.A). We then present the shape and an overview of a lipid membrane under indentation (in section III.B). The conformational transition of the lipid membrane and other related internal properties are studied in section III.C. The force−indentation curves are calculated in section III.D. The conclusions are given in section IV.

II. SIMULATION MODEL AND SETUP

Our system consists of lipid molecules, solvent molecules, and a hydrophobic thin supporting substrate. A pore of nanometer size is opened through the substrate, and the lipid molecules are spread across the pore, from the top and bottom sides of the substrate. Because of the hydrophobic interaction, the lipid

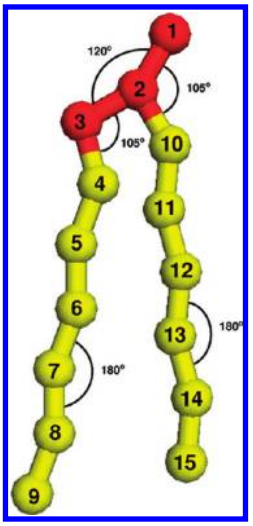

Figure 1. Schematic diagram of a lipid model. The red beads represent the lipid headgroup. The yellow beads represent the lipid tails. The values of θ_0 are indicated in the diagram.

molecules self-assemble into a bilayered structure, spanning and suspending over the pore. Outside the pore region, the two lipid monolayers sandwich the substrate. The mechanical properties of this pore-spanning lipid bilayer are then studied by indentation with a tip from the top middle of the pore to imitate a real experimental probing, for example, by AFM.

Simulating such a system by all-atom model simulations in which the details of the composed atoms are included and every condition of the experiments is respected is nearly impossible because the model contains an enormous number of atoms, which generally requires lots of computing resources and exceeds the power of most of today's computers to handle it. To overcome this difficulty, a coarse-grained approach, which groups certain atoms into new interaction units, is used in this study. Moreover, a quasi-2D method is employed in which only a thin slice of the pore-spanning lipid bilayer is simulated. The thin slice models the lipid system transected through the center of the pore. The thickness of the slice is chosen to give lipid molecules degrees of freedom to move, even in the direction of the thickness. A periodic boundary condition is applied in the x, y, and z directions to span the modeling system to a 3D case. The above two approaches significantly reduce the number of interaction sites of the system, and the simulations become feasible by today's computing power. The detailed setup of the system is described in the following text.

II.A. Lipid Molecule. In the coarse-grained model, neighboring atoms in a lipid molecule are grouped into new units, represented by beads, in a way that maintains the fundamental structure of a lipid, as shown in Figure 1.

A lipid molecule is modeled as a bead−spring double-tailed molecule. The head of the lipid molecule is composed of three hydrophilic beads, and each tail of the lipid is composed of six hydrophobic beads. All bead pairs interact through truncated and shifted Lennard-Jones (LJ) potentials

$$U_{\mathrm{LJ}}^{\mathrm{shifted}}(r) = \begin{cases} u_{\mathrm{LJ}}(r) - u_{\mathrm{LJ}}(r_c), & r \le r_c \\ 0 \quad , & r > r_c \end{cases} \tag{1}$$

where r is the distance between two beads and $u_{\mathrm{LJ}}(r) = 4\varepsilon[(\sigma/r)^{12} - (\sigma/r)^6]$. LJ parameters σ and ε denote the bead diameter and the strength of interaction, respectively. We assume that σ and ε are identical for all pairs of beads. For tail−tail bead interactions, the cutoff r_c is chosen to be 2.5σ, which includes the attractive interaction of the LJ potential. On the contrast, for head−head and head−tail pairs of interactions, r_c is set to $(2)^{1/6}\sigma$; in this case, the LJ potential is purely repulsive. This setup models the amphiphilicity of a lipid molecule. The reason that we do not include the attractive interaction in the head−head pair interaction is to avoid the unphysical wrinkling occurring on the surface of the lipid membrane because of the use of the phantom solvent model described below.[11] The beads in the lipid molecule are connected and form the chemical structure shown in Figure 1. The bead−bead connection is modeled by the finitely extensible nonlinear elastic potential

$$U_{\mathrm{bond}}(b) = -\frac{1}{2}kb_{\max}^{\ 2}\ln\left[1 - \left(\frac{b}{b_{\max}}\right)^2\right] \tag{2}$$

where b is the bond length, $b_{\max} = 1.5\sigma$ is the maximum bond length, and $k = 30\varepsilon/\sigma^2$ is the spring constant. This choice of parameters can avoid unlimited bond extension and crossing. Bond angle potentials are incorporated into the model through a harmonic form

$$U_{\mathrm{angle}}(\theta) = k_a(\theta - \theta_0)^2 \tag{3}$$

where θ is the angle between two adjacent bonds and $k_a = 2\varepsilon/\mathrm{rad}^2$ is the bending constant. There are three θ_0 values in our lipid model: $\theta_0 = 120°$ for bead triplet 1−2−3, $\theta_0 = 105°$ for bead triplets 2−3−4 and 1−2−10, and $\theta_0 = 180°$ for the other triplets in the tails, followed by the bead labeling in Figure 1. Each bead in our coarse-grained model represents a group of chemical atoms. A sketch of the coarse-graining mapping can be found in ref 50. Moreover, the choice of these parameters generates a persistence of about 2σ for the tail chains, which corresponds to that in a typical DPPC or DMPC lipid molecule.[10] A similar model has been used to study the properties of bilayer membranes[10] and the fusion between two liposomes.[7]

II.B. Solvent Molecule. The solvent environment is simulated by explicit solvent beads. A bead represents one cluster of three water molecules.[10] To avoid the immaterial problem of solvent structure and reduce the simulation time,[51] the phantom solvent model is employed in this study.[6,11] The computation time is largely saved through working with this model. In this model, the solvent beads do not interact with each other but interact with other beads in the simulation box, including the head and the tail beads of the lipid molecules, the beads that constitute the substrate and the indenting probe, via the purely repulsive LJ potential given in eq 1 with $r_c = (2)^{1/6}\sigma$. Note that the model does not allow momentum transfer between solvent molecules.[44] The hydrodynamic effect is hence not properly considered. Nonetheless, recent studies have shown that some hydrodynamic characteristics, especially the conservation of momentum, are very important in the simulations of membrane structure to produce the undulations of lipid membranes correctly.[16,50] Our solvent model holds this crucial characteristic well. The same models have been successfully used in many simulations to study the phase and structural transitions of lipid membranes under tension.[6,11,44] Of course, hydrodynamics could bring about some unexpected effects to the system, which can be justified only when it is implemented appropriately. Recent developments have allowed the hydrodynamics to be effectively simulated,

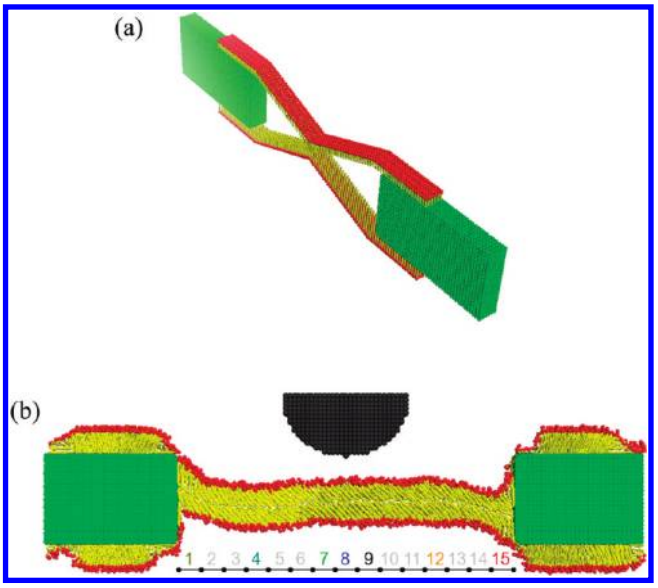

Figure 2. (a) Initial configuration. (b) Snapshots of the system before indentation. The red and yellow beads represent the headgroups and the tails of the lipid molecules, respectively. The green beads constitute the pore substrate, and the black ones, the hemisphere probe. The solvent beads in the picture are not shown for clarity. The lipid molecules are initially placed into two layers that finally sandwich the substrate across the pore when the system is equilibrated. The pore is divided into 15 regions, as indicated in b. In section III, we will study the local structure of a lipid membrane in these regions.

for example, by dissipative particle dynamics[52,53] or by multiparticle collision (MPC) dynamics.[54,55] In particular, the MPC dynamics differ in our simulations by additional collision steps, after streaming steps, which permit the momentum transfer between solvents. However, these collision steps require more computing efforts. Because our resources are limited, we will not use MPC dynamics in this study. Regarding the fact that momentum conservation is held in our model, we do not expect significant changes in our results if MPC dynamics is implemented.

II.C. Substrate and Probe. The substrate and the probe consist of beads. The beads form a simple internal cubic lattice structure, with a lattice constant equal to 1σ. In our quasi-2D model, the nanopore is represented by two rectangular blocks of substrates located separately on the left- and right-hand sides of the simulation box (See the initial configuration in Figure 2a.) The distance between the inner edges of the two blocks is the diameter of the pore and is set to 80σ. The thickness of the substrate is 20σ, and the width of each block is 30σ. We consider the case in which the substrate surface is hydrophobic. The substrate beads interact with the lipid tail beads through the attractive version of eq 1 with $r_c = 2.5\sigma$. They interact repulsively with the other beads. The probe is shaped as a hemispherical body, and the radius of the hemisphere is 15σ. It is used in the study of indentation. The probe beads interact repulsively with other kinds of beads. In a real case, there can be adhesion between the probe and the lipid and solvent molecules.[45,56] There is also the proposal that solvent extrusion can give rise to extra attraction.[57] The hydrophobic or hydrophilic character of the probe has been shown to affect the details of the membranes under indentation or intrusion.[45,47,49,56] Nonetheless, in this study, we pay more attention on the pure response of the lipid membranes to the indenting force. The attractive force with the probe is ignored. Therefore, no adhesion between the probe and lipid membranes and solvent is considered.

Table 1. Summary of Interactions among Lipid Head Beads, Lipid Tail Beads, Solvent Beads, Substrate Beads, and Probe Beads[a]

bead−bead	head	tail	solvent	substrate	probe
head	R	R	R	R	R
tail	R	A	R	A	R
solvent	R	R	X	R	R
substrate	R	A	R	X	R
probe	R	R	R	R	X

[a] The notation R means a repulsive interaction given by eq 1 with $r_c = (2)^{1/6}\sigma$. The notation A means an attractive interaction given by eq 1 with $r_c = 2.5\sigma$. X means no interaction.

A summary of the interactions among different types of beads used in this simulation can be found in Table 1.

We place 570 lipid molecules and 27 530 solvent beads in a simulation box of size $140\sigma \times 6\sigma \times 50\sigma$. The smallest side of the simulation box (in the y direction) allows three lipid molecules to fit in, side by side. Because the periodic boundary condition is applied, our quasi-2D model simulates a system with infinite replicas. Therefore, the 3D effect has been largely taken into account. The density of the solvent corresponds to the water density under ambient conditions. The simulations are performed in the NVT ensemble using the Nosé−Hoover thermostat.[58,59] The equations of motion are solved with the Verlet integrator using simulation package LAMMPS.[60] The integration time step Δt is 0.005τ, where $\tau = \sigma(m/\varepsilon)^{1/2}$ is the time unit and m is the mass of a bead. The temperature T is set to $0.9\varepsilon/k_B$, except in section III.A in which T is varied to study the phase behavior, where k_B is the Boltzmann constant. Initially, the lipid molecules are positioned into two layers with the lipid tails pointing inward, forming a joint in the middle of the pore as shown in Figure 2a. After about 10^7 MD equilibration steps, the lipid molecules form a bilayered structure that is suspended across the pore. We will show in section III.A that the lipid membrane is in the gel phase at this temperature. In the study of indentation, the probe is placed in the solvent region where the solvent beads have been removed. The initial position of the probe is at the center, 10σ above the middle plane of the pore (Figure 2b).

After equilibration, the probe moves downward at a speed of $0.001(\sigma/\tau)$. The indentation process runs for 10^7 MD steps. In the final stage of the process, the probe pierces the membrane. Five independent runs were performed in this study to obtain an average and a check of the consistence. The simulations were run on a homemade PC cluster. A typical indentation run takes about 400 h of CPU time. In our model, σ and τ correspond to a real length of about 0.46 nm and a time of 2.1 ps, respectively. Therefore, we simulate a membrane suspended on a 37-nm-diameter nanopore. Here, the speed of indentation is very large, several orders of magnitude faster than the typical speed used in experiments. This is a typical problem encountered in steered MD simulations because of the limitations of today's computing power.[47,49] Despite the fast indentation rate used here, the response of the lipid membrane in our study exhibits elastic behavior similar to what has been observed in experiments with a low rate.[34] Therefore, our simulations can qualitatively capture

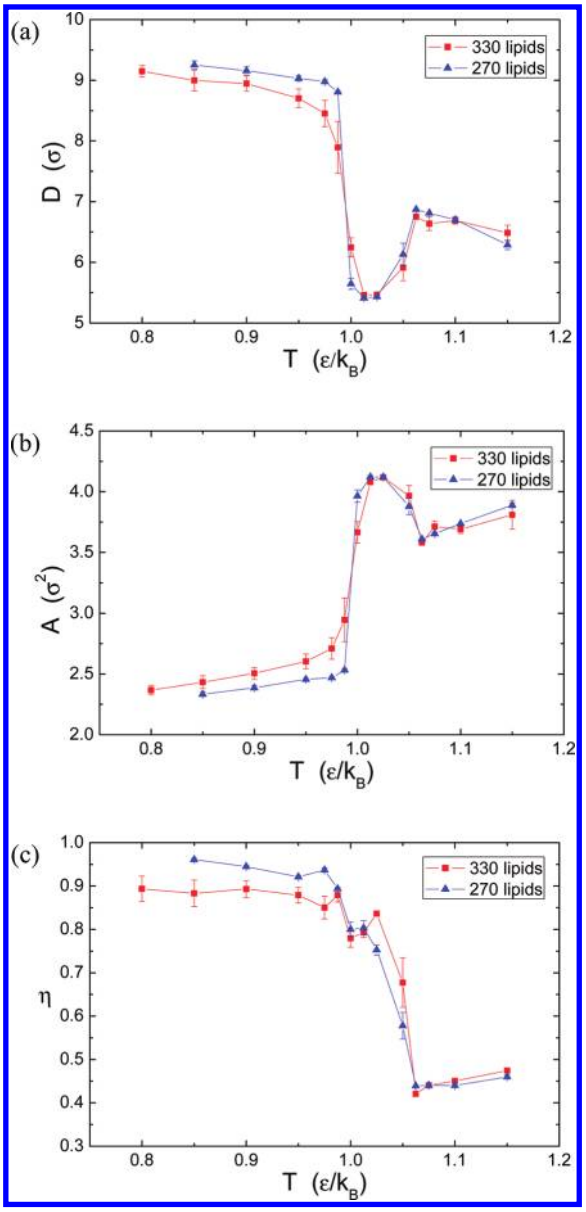

Figure 3. (a) Membrane thickness D, (b) area per lipid A, and (c) nematic order parameter η as a function of temperature T. The results for the system with 330 lipid molecules and that with 270 lipid molecules are plotted in red and blue curves, respectively.

the properties of a real system. For the first simulation study of the indentation of the system, we concentrate on the generic behavior and phenomena revealed at the molecular level by the indentation.[61] To shorten the notation, in the following text all of the physical quantities will be reported in a reduced unit system in which the length unit is σ and the energy unit is ε. For example, the strength of the force is reported in units of ε/σ.

III. RESULTS AND DISCUSSION

III.A. Phase Transition of a Lipid Membrane in Bulk Solutions. Before entering into the main topics of study in the indentation of a suspended lipid membrane, we study first the phase behavior of lipid membranes in bulk solutions in order to justify the setting of our model.

The systems were run in an isothermal−isobaric ensemble using a Nosé−Hoover barostat with a pressure setting of 1.0.[62] The initial size of the simulation box was chosen to be $100 \times 6 \times 40$. Because the dimension in the y direction is very small compared to those in the x and z directions, the system can be regarded as a quasi-2D system. Lipid molecules were initially positioned at the lattice points of a two-layered hexagonal lattice with the headgroup of the lipids pointing outward. Two systems consisting of different numbers of lipid molecules, 270 and 330 lipids, were simulated. Solvent beads (9000) were added to the two systems. Each system was run at several temperature points ranging from 0.8 to 1.15. It took about 10^7 simulation steps to get the systems equilibrated.

After equilibration, we collected data for the following 2×10^7 steps to calculate the membrane thickness, area per lipid, and nematic order parameter to study the structure and the phase of the lipid bilayer. The membrane thickness is defined to be the average vertical distance between the surfaces of the first tail beads in the upper and lower leaflets of the bilayer. The first tail beads are labeled as 4 and 10, as shown in Figure 1. The area per lipid is calculated by dividing twice the cross section of the system in the xy plane by the number of lipid molecules. The tensor of nematic order in a studied region of space is calculated by

$$S_{\alpha\beta} = \frac{1}{2N_l}\sum_{n=1}^{N_l}(3\ell_{n\alpha}\ell_{n\beta} - \delta_{\alpha\beta})$$

where the sum runs over all of the N_l lipid molecules in the region, $\ell_{n\alpha}$ and $\ell_{n\beta}$ are, respectively, the α and β components of direction vector $\vec{\ell}_n$ of the nth lipid molecule, α and β stand for the vector components (x, y, or z) in Cartesian coordinates, and $\delta_{\alpha\beta}$ is the Kronecker delta.[63] The direction vector $\vec{\ell}_n$ is calculated by averaging the two tail vectors $\overrightarrow{r_9r_4}$ and $\overrightarrow{r_{15}r_{10}}$, in Figure 1, of a lipid molecule. The tensor was calculated from simulations, and three eigenvalues of the tensor were computed. The largest eigenvalue is called the nematic order parameter.[11] The largest possible value of the nematic order parameter is 1, which results from a perfect arrangement of the direction vectors pointing parallel to each other. The value 0 is derived from a complete randomization of the vectors.[63] The results for the membrane thickness D, the area per lipid A, and the nematic order parameter η versus temperature T are shown in Figure 3a−c, respectively. Red curves are the results obtained from the system of 330 lipid molecules, and blue curves illustrate the system of 270 lipids.

We can see that the lipid membrane system exhibits, in turn, three phases at increasing temperature. When the temperature is less than 1.0, the lipid membrane shows bilayer structure with a thickness of around 9σ and an area per lipid of around $2.5\sigma^2$. The nematic order parameter is about 0.9, which is close to 1, showing the good alignment of the lipid molecules. The system is hence in a gel phase. With T rising to over 1.0, a drastic decrease happens in the thickness whereas the nematic order parameter is still high. It indicates the formation of the interdigitated gel phase, characterized by a small thickness of about 5.5σ and a large area per lipid of $4.25\sigma^2$. Between the gel phase and interdigitated gel phase, a two-phase coexistence was observed. In this region, the membranes are partially in the gel phase and partially in the interdigitated phase. When T is larger than 1.05, the state of the liquid-crystalline phase was observed. In this phase, the lipid membrane has a thickness of about 6.5σ and an area per lipid of $3.75\sigma^2$. The thickness is greater than that in the interdigitated gel

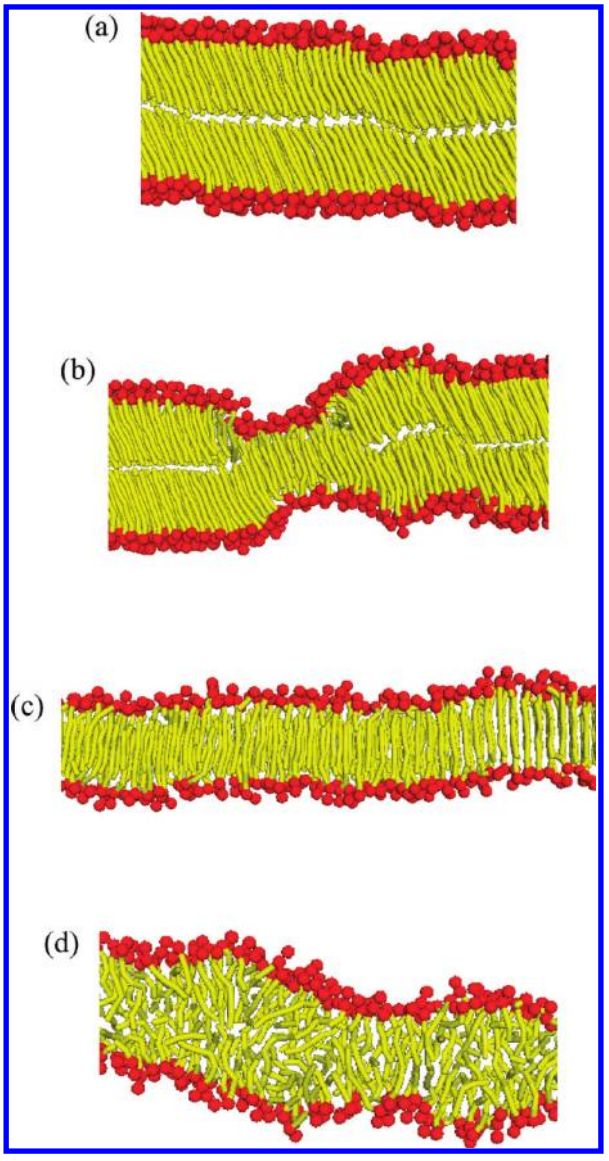

Figure 4. Snapshots of membrane in (a) the gel phase (T = 0.9), (b) two-phase coexistence (T = 0.975), (c) the interdigitated gel phase (T = 1.025), and (d) the liquid-crystalline phase (T = 1.1). The representation of the picture is the same as described in the caption of Figure 2.

phase, but the area per lipid is smaller. More importantly, a small nematic order of around 0.4 is observed, showing that the tails of the lipid molecules are arranged in a very random way inside the bilayer structure. The area per lipid obtained in our simulations corresponds to real values of 53, 90, and 79 Å^2 in the gel, the interdigitated gel, and the liquid-crystalline phase, respectively. The results are in agreement with experimental findings[64,65] and simulations.[10]

To give readers a clear picture, we present in Figure 4 snapshots of a membrane in the gel phase, the two-phase coexistence, the interdigitated gel phase, and the liquid-crystalline phase. We can see clearly that a bilayered membrane changes its structure to the interdigitated gel state and then to the disordered liquid state as the temperature increases.

In the gel phase, we also observed that the lipid molecules have a tilting-angle preference. This is essentially due to the large asymmetric headgroup in our lipid model. The lipid molecules,

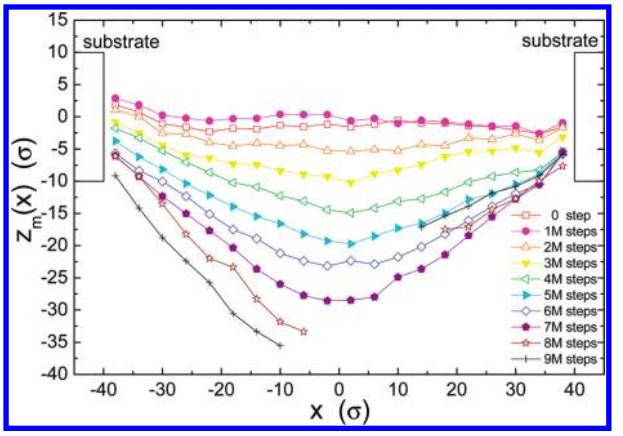

Figure 5. $z_m(x)$ at different simulation moments for each 1 M time step.

commonly used in experiments such as DPPC and DMPC, do show this tilting tendency in the gel phase at low temperature. The tilted gel phase plays an important role in the determination of the bending mechanism of a suspended lipid bilayer, as we will show in section III.C.1. The tilt angle obtained here is 26 ± 7° with respect to the membrane normal, which agrees fairly well with experiments[66] and simulations.[12] We have tested the tilting angle dependence on the balance between head-bead repulsion and tail-bead attraction by varying the head-bead repulsion strength from 0.1ε to 5ε and have found that the tilt angle increases insignificantly from 23 to 27°. This is because the structure is mainly determined by the balance between the size of the lipid headgroup and the tails. To be a general model, we simply set the strength ratio for the head-bead repulsion and tail-bead attraction to be 1:1. This setup is also similar to the setup used by other simulation groups.[7,10,11,44]

The phase behaviors shown here are consistent with those found in real experiments[64,65] and other simulations.[6] The model also vitally captures the titling-angle feature of lipid molecules in membranes. These characteristics support the validity of our simulation model. However, we stress that the aim of this work is to provide a general understanding of the behavior and mechanism of a membrane system under indentation through a simple coarse-grained model. Pursuing quantitative agreement for every physical quantity is not our goal and is also impossible.

III.B. Global Structure of Suspended Lipid Membrane under Indentation. We now go back to the main topic: studying the indentation of a lipid membrane suspended across a nanopore. The temperature T is fixed at 0.9, where the system is in a gel phase. Under indentation, the shape of the membrane deforms and varies with time. To understand this deformation, we calculated the z coordinate of the middle line of the membrane sheet at every point in the pore. This quantity is denoted by $z_m(x)$, where x is the position across the pore region. The results at different simulation moments are presented in Figure 5. Each curve displays the membrane shape at a specific time.

We observed that the shape function $z_m(x)$ is not exactly a horizontal line before the indenting probe contacts the membrane. It inclines toward one side of the pore. This inclination occurs because the constituted lipid molecules are not perpendicular to the bilayer when the bilayer is formed. In this situation, the forces exerted on the lipid molecules by the attraction of the pore edges from the two sides shear the membrane in the vertical direction, resulting in an inclined membrane as shown in the

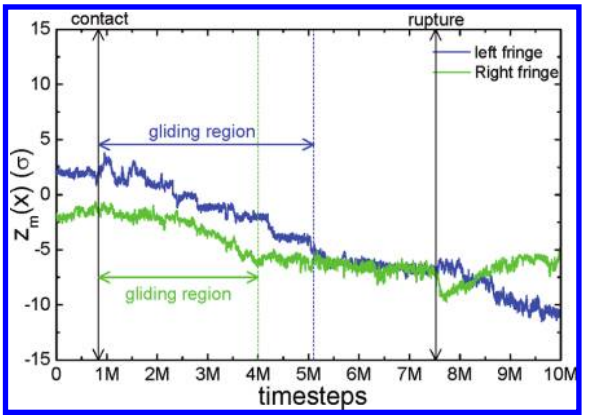

Figure 6. Time evolution of $z_m(x)$ at left and right fringes of the membrane, plotted in blue and green, respectively. The right fringe stops gliding at around time step 4.0M, and the left one, at around 5.1M.

snapshot of Figure 2b. As time passes, the probe descends. Once it touches the membrane, the membrane starts to deform. The process takes place in two ways: bending and downward gliding. Bending occurs in the middle of the membrane, where the probe makes contact with it. Gliding occurs at the two edges of the pore where the membrane moves downward with time. Simulation time step 0.8M to 5.1M (M stands for one million) in Figure 5 refers to this process. Gliding stops when $z_m(x)$ approaches the bottom edge of the pore. Because of the inclination, the right fringe of the membrane stops gliding at time step 4.0M, earlier than does the left fringe.

We plot in Figure 6 the time evolutions of $z_m(x)$ at the left and right fringes of the membrane. We saw that the two curves exhibit a step-by-step descending behavior, particularly for the left fringe, which shows that the gliding of the membrane happens intermittently, dropping down suddenly at specific points. Although the probe keeps pushing the membrane downward, the fringes of the lipid membrane remain fixed at a certain position until the stored stress is large enough to overcome the threshold value, which is the maximum frictional force required for the lipid molecules to glide on the pore edge. Mey et al. have reported a similar stairlike descending behavior in the force indentation curves in their experiments.[34]

When the two sides of the membrane both reach the bottoms of the pore edges, the membrane stops gliding. The only way to proceed is via bending. (See time steps 5.1M to 7.5M.) The strain increases with time, and the membrane becomes more and more arched. When the indentation becomes deep enough, an abrupt rupture takes place because the strain exceeds the mechanical threshold of the membrane and the membrane is cut into two pieces (Refer to time step 7.5M.) We present snapshots of the time evolution of the membrane in Figure 7. These pictures, from top to bottom, show three stages of shape variation for the suspended membrane under indentation: (I) gliding and bending, (II) purely bending, and (III) rupture.

III.C. Internal Structure of a Suspended Membrane under Indentation. After having studied the global structural change of the lipid membrane under indentation, we now go inside the membrane and investigate its internal structural change and the local organization of the constituent lipid molecules. We divided the pore into 15 regions along the x direction, as indicated in Figure 2b. Regions 1 and 15 are the two fringe regions where the membrane is in contact with the pore edges; region 8 is the middle region where the probe indents the membrane. We calculate the following structural quantities.

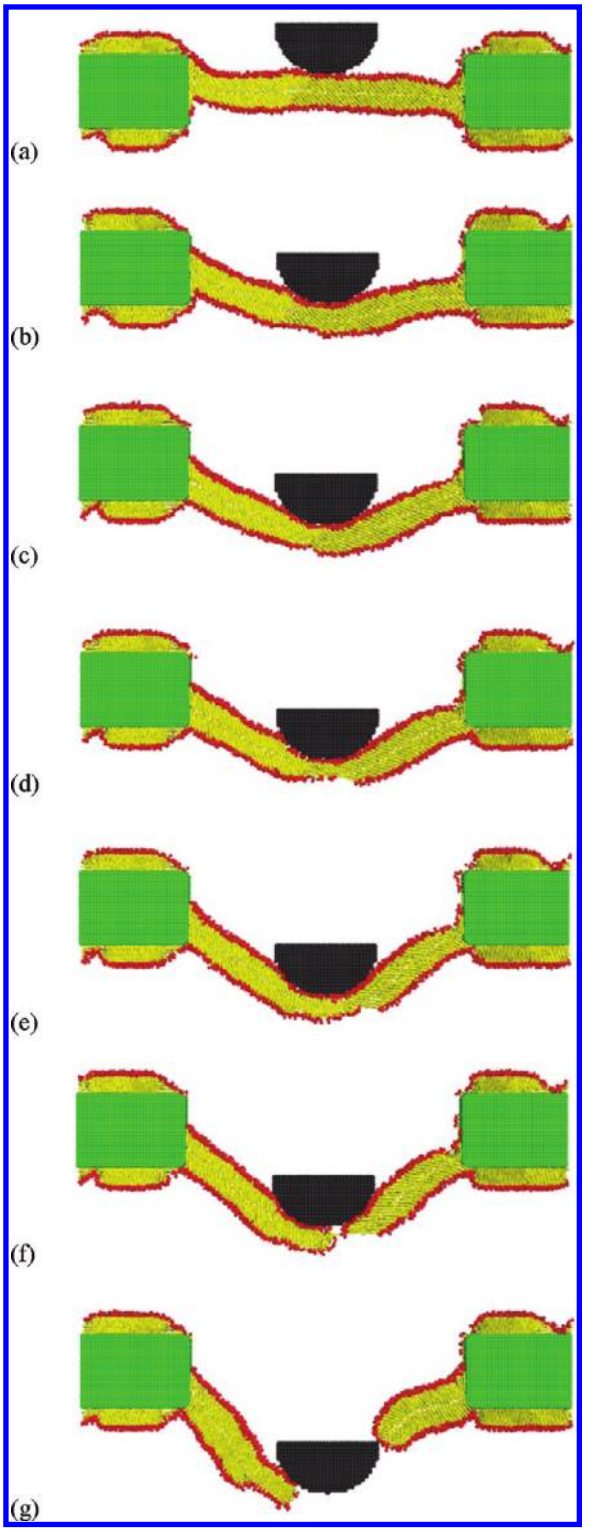

Figure 7. Snapshots of the membrane system under indentation at several timesteps: (a) 1M, (b) 4M, (c) 5.5M, (d) 6M, (e) 7M, (f) 7.5M, and (g) 9M. The representation of the picture is the same as described in the caption of Figure 2.

III.C.1. Tilt Angle of a Lipid Molecule. The tilt angle θ of a lipid molecule is defined to be the acute angle between the lipid direction vector $\vec{L}$ and the z axis. The z axis is perpendicular to

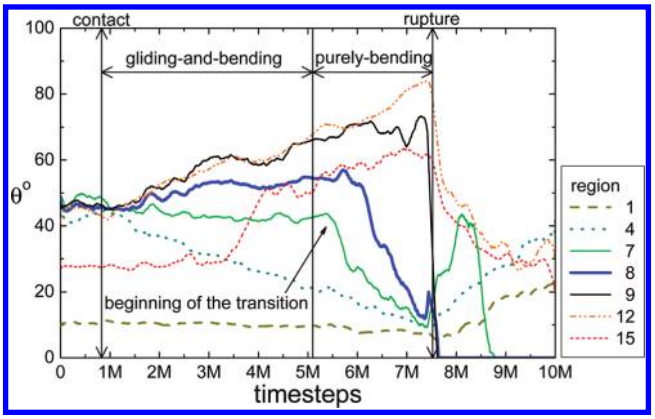

Figure 8. Time evolution of the tilt angle θ of lipid molecules in different pore regions.

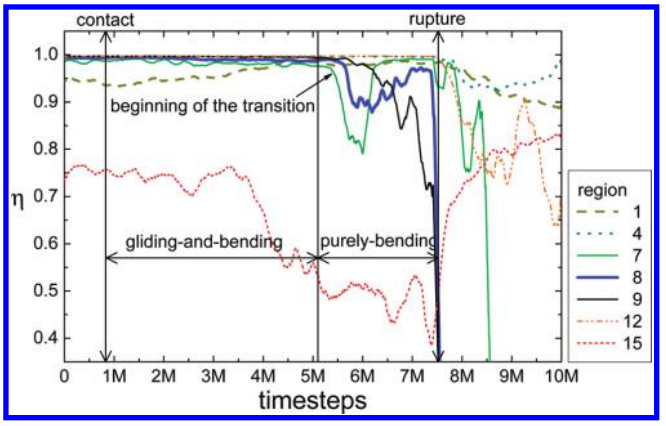

Figure 9. Time evolution of the nematic order parameter η in different pore regions.

the pore−substrate plane in this study. The moving direction of the indenting probe is downward, following the $-\hat{z}$ direction. How the tilt angle changes with indentation in different pore regions is plotted in Figure 8.

We observed that before the indenting probe touches the membrane the tilt angle of the lipid molecules is about 45° in the internal regions of the membrane (from region 2 to 14), with an angle fluctuation of about 10°. This tilt angle is slightly larger than that in bulk solutions (∼35°) obtained by experiments[66] and simulations.[12] It is known that our membrane is subjected to a lateral tension due to the attractive force of the substrate, which pulls the membrane outward from the two pore edges. It renders a lying-down effect on the lipid molecules, in contrast to the membrane in a bulk solution. The lipid molecules thus acquire a larger tilt angle to balance this extra tension. However, in regions 1 and 15, θ is 10 and 27°, respectively. The hydrophobicity of the substrate attracts the lipid tails, which renders the lipid molecules lying parallel to the wall edges of the pore, resulting in a small value of θ. In the course of the indentation, asymmetric behavior in the angular variation with time was observed: the tilt angle decreases against the indentation for the left regions of the lipid membrane (from region 1 to 6) but increases for the right regions (from region 9 to 15). The physics can be understood as follows. Because of the unique tilting direction of the lipid molecules, the left part of the suspended membrane suffers a shearing strain by the probe indentation, which shears the membrane along the lipid direction. The lipid molecules thus rotate clockwise, leading to a decrease in θ. In contrast, the right part of the membrane suffers a bending strain, which bends the membrane in a similar way to extending an accordion's bellows left downward. Hence, the lipid molecules in this part rotate counterclockwise, and θ increases. In the middle regions of the membrane (regions 7 and 8), the lipid molecules tend to maintain their tilt angles against the indentation. Nonetheless, the angle shows an abrupt change, starting at some point in the purely bending stage. We will explain this phenomenon later.

θ in the two fringe regions, regions 1 and 15, does not show a significant change in the gliding-and-bending stage. Membrane gliding can decrease the stress of the indentation and hence reduce the deformation. This effect is important in the maintenance of the stability of the lipid membrane, particularly in the early stage of indentation, to avoid rupture due to large stress and strain.

We remark that many membrane systems comprise lipid molecules with a tilting angle.[16,66−68] Our simulations predict an interesting asymmetrical local structural change upon indentation for such systems. There are also membranes that are made of nontitled lipid molecules.[15,16] For these systems, the response to the indentation is expected to be different. It is worth being investigated in the future.

III.C.2. Nematic Order Parameter. To understand the degree of local arrangement of lipid molecules in the suspended membrane, we calculated the nematic order parameter η by the method described in section III.A and studied its variation with time. The results in different pore regions are presented Figure 9.

We observed that in the gliding-and-bending stage, η takes a value very close to 1 for all of the regions except the two fringe regions. It suggests a regular arrangement in the interior of the membrane in which the lipid molecules tend to align parallel to each other. For the lipids in the fringe regions, the molecules also interact with the hydrophobic walls of the pore, which perturbs the alignment. Consequently, the arrangement is less ordered. Please notice that η in the right fringe, region 15, shows decreasing behavior, starting at a time step of ∼4.0M. This behavior occurs because the membrane fringe stops gliding when it arrives at the bottom corner of the pore, and some of the lipid molecules traverse into the lower surface of the substrate, which results in a decrease in the ordering. However, the left fringe of the membrane (region 1) stops gliding at a later moment (at a time step 5.1M). The tilting direction of the lipid molecules on this side is more parallel to the pore wall, which prevents the traversing of the lipid molecules into the lower substrate surface. Therefore, the ordering stays high.

At the purely bending stage of indentation, a drastic change was observed: the values of η in regions 7−9 decrease suddenly at some moment and return to 1 after a while, exhibiting a valleylike curve. This drastic change suggests the occurrence of a structural transition inside the membrane. During the indentation process, the lipid membrane suffers an increasing bending strain by the indenting probe. Gaps eventually occur in the middle of the membrane between the lipid molecules along the x direction and grow with time. Because the lipid molecules have more room to fluctuate, the ordering in these regions decreases. When the gap size is large enough, the interpenetration of the lipid molecules in the upper leaflet into the lower leaflet becomes allowed, promoted by the intermolecular interaction. The

bilayered structure is reassembled into an interdigitated, monolayer structure. This interdigitated layer is a highly ordered structure. Consequently, the order parameter grows back to 1. The structural transition from a bilayered structure into an interdigitated monolayer extends the lateral dimension of the membrane significantly, which indispensably decreases the stress of indentation and prolongs the lifetime of the membrane against the final rupture. A similar stress-induced phase transition has been reported in simulation studies.[44] Neder et al. found that lipid membranes in the liquid-crystalline phase and in the ripple phase can partially or completely transit into an interdigitated phase under surface tension, but not in the gel phase. In our simulations, the probe indents the lipid membrane constantly. The stress can be very large, which leads to the occurrence of such a phase transition even from a gel phase.

In our study, the purely bending stage can be further divided into three phases, depending on the internal structure of membrane: (1) a bilayer phase, (2) a transient phase, and (3) an interdigitated-layer phase. These three phases occur at different time points of indentation for different regions of the membrane. We can see from the snapshots in Figure 7 how these three phases take place one after another. We observed that the phase transitions start at region 7 and propagate to neighboring regions 8 and 9. The three regions are the most stressed regions on the membrane because they suffer the direct indentation of the probe there. The propagation of the phase transitions can be seen in Figure 9, where the value of η in regions 7−9 exhibits, in turn, a valleylike curve. When the bilayered structure transforms locally into the interdigitated-layer structure, the lipid molecules inside line up again in a parallel fashion. Moreover, the direction of the lipid molecules gradually becomes more perpendicular to the pore, as recorded in Figure 8 where the tilt angle θ decreases after the occurrence of the phase transition in the regions. The calculated value of θ shows that at the moment before the rupture of the membrane, the lipid molecules in these central regions are basically normal to the surface.

The phase transition of the lipid membrane under indentation has been observed in experiments. Simon et al. found that a part of the sample of lipid membranes in a nanopore in their experiments was irreversibly deformed, which can be attributed to the phase transition found in our simulations.[20] Besides, another experiment performed by Mey et al. also revealed some features of the phase transition.[34] This will be discussed in section III.D.

III.C.3. Included Angle between Neighboring Lipid Molecules. The occurrence of the phase transition from a bilayered structure to an interdigitated one can be identified by studying the included angle between neighboring lipids. Two kinds of included angles were calculated. The first one, denoted by ϕ, is obtained by calculating the acute angle between neighboring lipid molecules without considering their vector directions. The second one, denoted by φ, is calculated, on the contrary, by considering the vector direction of the neighboring molecules. Therefore, φ takes a value ranging from 0 to 180°. Because the lipid molecules in the upper and lower leaflet of a bilayered membrane are locally parallel to each other, the value of φ is expected to be 0°. For an interdigitated membrane, the neighboring lipids are antiparallel and hence the value of φ should be 180°. However, we expect that ϕ takes a value of 0° in both cases. The mean values of ϕ and φ as a function of time in different pore regions are presented in Figure 10a,b, respectively.

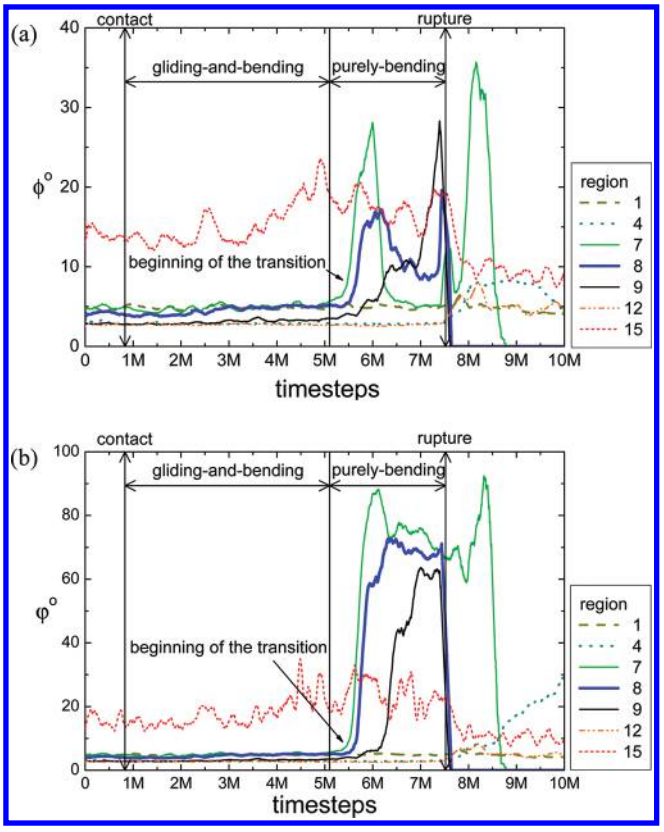

Figure 10. Time evolution of included angles (a) ϕ and (b) φ between neighboring lipid molecules in different pore regions.

We can see that ϕ is a constant at the gliding-and-bending stage of indentation in each pore region. It begins to increase when the indentation enters into the purely bending stage. This increase starts in the middle regions of the membrane and propagates gradually toward the edge regions. As we have seen in the previous subsection, the strain due to the indentation can become very large and eventually trigger a structural transition inside the membrane to reduce the strain. What we can see in Figure 10a is that ϕ in the middle regions shows an abrupt increase and decrease in the purely bending stage. These abrupt changes correspond to the same moments when the tilt angle θ (in Figure 8) starts to decrease.

The value of φ in regions 7−9 also rises suddenly at the same time (Figure 10b). It then maintains a value between about 70 and 90° whereas ϕ drops back to a small value of about 5°. This information, together with that obtained in the calculation of the ordering parameter ($\eta \approx 1$) in Figure 9, shows the internal structural change from an ordered (bilayer) structure to another ordered (interdigital) structure under the indentation. One question has to be answered: Why is the value of φ not 180° after the transition, as we expect? The reason is that in our quasi-2D system the suspended membrane suffers tensional strain only in the x direction (across the pore) but not in the y direction. As the probe goes down, the indenting tension causes an increase in the separation distance of the neighboring lipid molecules in the x direction. The increase in the distance eventually allows the docking of the upper leaflet of the bilayered membrane into the lower leaflets. The interdigitated structure is therefore formed along the x direction but not along the y direction. Therefore, a lipid molecule has only about half of its neighbors parallel to it

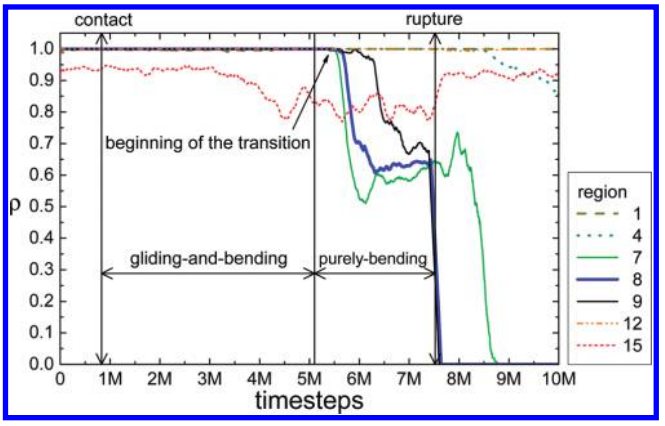

Figure 11. Time evolution of the same-direction percentage ρ in different pore regions.

and half of them antiparallel. To confirm this picture, we calculated the percentage ρ of the neighboring lipids parallel to a surrounding lipid molecule. The results are shown in Figure 11.

We found that ρ is a constant and very close to 100% at the beginning. It agrees with the results of small values of ϕ and φ. At the moment when the structural phase transition takes place (where ϕ and φ drastically increase), ρ decreases quickly, down to a value of about 60%, and is maintained at this value before the rupture of the membrane. The result clearly shows that the neighboring lipid molecules are partially parallel and partially antiparallel to the surrounded lipid, as we depicted. Because only about 40% of the neighboring lipids are antiparallel, the included angle φ is estimated to take a value of $0° \times 60\% + 180° \times 40\% = 72°$, which is consistent with the result shown in Figure 10b.

It is worth noticing that in a real 3D system a suspended lipid membrane can suffer lateral tension from the pore rim in both the x and y directions. Consequently, the interdigitating of the lipid molecules could happen in the two directions upon indentation and propagate outward from the indented center. The above studied quantities are thus expected to show a pattern depending on the tilting direction of the lipid molecules. This interesting phenomenon can be studied only when a true 3D model of the membranes spanning over pores is used. It deserves further investigation in the future.

III.C.4. Distance between Neighboring Lipids. During the indentation process, the membrane is bent in the middle and the tensional force causes the extension of the lateral dimension of the membrane. As discussed in the previous subsections, this extension enlarges the separation distance between neighboring lipids, which plays an important role in the determination of the internal structure of the membrane. To understand this effect quantitatively, we investigated here the separation distance between neighboring lipids. The distance is defined to be the mean distance between the centers of mass (CM) of two neighboring lipids. It can be split into two components. One is the normal distance, which is the distance normal to the direction of the lipid molecules. The other component is the shear displacement, which is the CM distance projected in the lipid direction. The former component describes the normal strain inside the membrane, and the latter evaluates the shear strain. The results for the normal distance and the shear displacement are presented in Figure 12a,b, respectively.

We can see that the normal distance in middle regions 7−9 increases in the course of indentation, up to the time step of ~5.4M. This increase creates gaps between lipid molecules in the

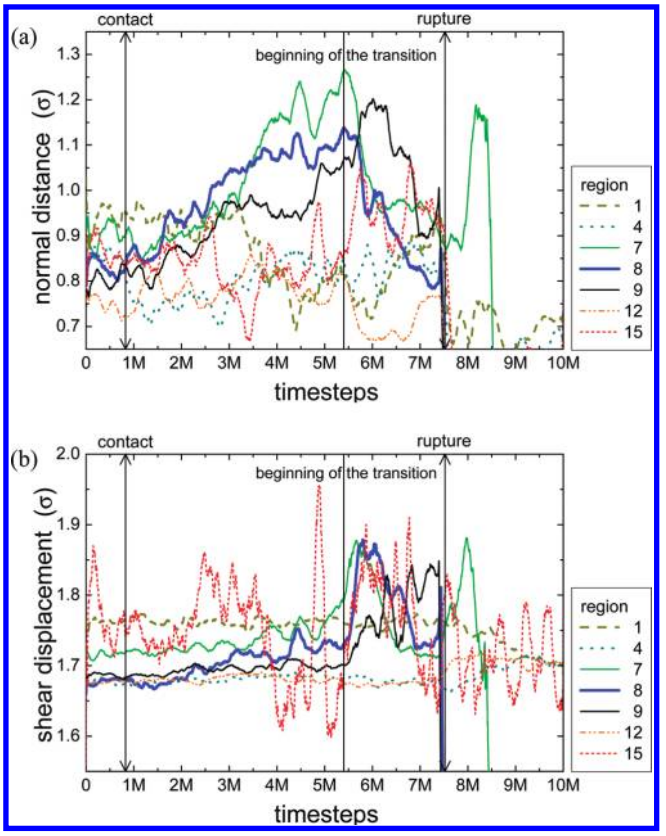

Figure 12. Time evolution of (a) the normal distance and (b) the shear displacement in different pore regions.

bottom leaflet of the membrane. When the gaps are large enough, the lipid molecules in the top leaflet of the membrane penetrate the gaps in the bottom leaflet, forming the interdigitated layer structure. Once the new structure is formed, the normal distance decreases and returns back to a value similar to that in the bilayered structure. Therefore, the curve of the normal distance exhibits a peak structure that marks the occurrence of the phase transition.

The calculation of the shear displacement in different pore regions shows that the shear displacement in the middle regions also reveals a peak structure associated with the phase transition. After the formation of the interdigitated phase, the shear displacement starts to decrease. This behavior can be associated with the decrease in the tilt angle of the lipid molecules in the well-ordered interdigitated layer shown in Figures 8 and 9. We also observed that region 7 is the region that first reaches the largest shear displacement and normal distance. Therefore, the phase transition takes place first in this region. Because the shear displacement is relatively small compared to the normal distance, it is the normal distance that determines the occurrence of the transition.

III.D. Force−Indentation Curve. Finally, we investigated the mechanical property of the system. The relationship between the force and the displacement of the indentation probe was studied, and the apparent spring constant was calculated from the slope of the force−indentation curve. The issue is of concern in many applications.

The force of the probe was computed by the reacting force of the lipid molecules acting on the probe. Only the z component of the force takes effect because the indenting probe moves

dx.doi.org/10.1021/la201977d |*Langmuir* 2011, 27, 11930–11942

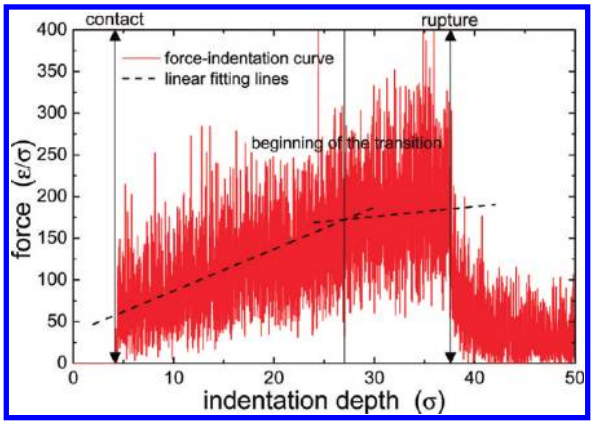

Figure 13. Force−indentation curve. Two linear regimes are identified before rupture of the membrane. The dashed lines show the slopes of the linear fitting in the two regimes.

downward along the z direction. The indentation depth is the descending distance of the probe counting from its position before indentation. The results, the force versus the indentation depth, are presented in Figure 13.

We observed that the force increases with the indentation depth after the probe contacts the lipid membrane. Two linear regimes were identified. The boundary of the two regimes is located at the moment when the phase transition to an interdigitated state takes place, at a time step of 5.4M, or equivalently, at the indentation depth of 27σ. The first regime has a slope much larger than the second one. The two slopes averaged from five independent runs yield values equal to $4.1 \pm 0.5\ \varepsilon/\sigma^2$ and $0.2 \pm 0.7\ \varepsilon/\sigma^2$, respectively, which correspond to apparent spring constants of 0.081 ± 0.009 N/m and 0.003 ± 0.013 N/m. The force suddenly decreases when the membrane is ruptured.

The elastic response of the membrane upon indentation generally comprises three contributions: bending, lateral tension, and stretching.[69] Bending makes a minor contribution to the apparent spring constant in the range of 0.01 mN/m, and the latter two are responsible to a large extent in experiments. The lateral tension gives rise a linear response, which is due to the adhesion and friction of the pore substrate on the suspended membrane. Stretching occurs when the indenting force is strong and is dominated by a cubic law of the force−indentation curve. Our results show a predominately linear dependence, particularly in the first regime. It is thus the lateral tension that dominates the behavior, as suggested by Mey et al.[34] Moreover, the value of the apparent spring constant depends very much on the hydrophobic/hydrophilic character of the pore substrate. On hydrophilic pores, the spring constant is small with a range of 0.2−2 mN/m, whereas on hydrophobic pores, it is large and the value stays in the range of 20−40 mN/m.[34,46,56] Our simulations show the same order of magnitude for the force constant.[34,45] In experiments, a nonlinear effect on the force−indentation curve has been observed but usually shows up as a weak contribution.[56] This effect can be explained by a generalized Canham−Helfrich model, which has been derived recently.[70] However, because of the fluctuations, the nonlinearity cannot be clearly seen in our study. Therefore, following the suggestion of Mey et al.,[34] we presumed to fit the regime with a linear equation to get the apparent spring constant.

Generally, a force−indentation curve can reveal information about the membrane structural transition in the indentation process. The first linear regime shows that the lipid membrane has an elastic response to the indentation. The second regime shows a reduction in the slope of the force−indentation curve, which indicates a change in the internal structure in the lipid membrane. As we have seen in section III.C, a local phase transition from a bilayerd structure to an interdigitated one does occur at this moment. It involves a rearrangement of lipid molecules, which increases the lateral dimension of the membrane upon indentation. This dimensional extension prevents an increase in stress inside the membrane; therefore, the apparent spring constant largely decreases. We note that in experimental and theoretical analyses of force indentation people usually do not consider any phase transition that changes the internal structure of the membrane. Our molecular simulations clearly show this possibility. The effect of the phase transition can be captured in the force−indentation curve by a reduction of the force constant. The data in the second regime of our figure does support this idea. Experiments have already observed a plateau or sawtoothlike behavior in force−indentation curves.[20,34] The behavior could be attributed to the consequence of an internal structural transition. The information obtained here provides a new direction in thinking and in the analysis of the membrane properties in the future.

IV. CONCLUSIONS

We have established a quasi-2D coarse-grained model for pore-spanning lipid membranes to investigate the mechanical properties of the system under indentation by a semispherical probe. The model has been verified by studying the membrane thickness, the area per lipid, and the nematic order parameter at different temperatures. Three phases of the lipid membrane have been identified: the gel phase, the interdigitated gel phase, and the liquid-crystalline phase. In the study of indentation, we have calculated the shape function of the lipid membrane. According to the variation of the shape function, the indentation process can be categorized into three stages: (1) gliding and bending, (2) purely bending, and (3) rupture. In the first stage, the membrane glides downward intermittently and stops gliding when the membrane fringes reach the bottom of the pore edges. Membrane bending occurs in the middle of the membrane because of the indentation of the probe. It takes place in the first and second stages and ends when the membrane is ruptured. We have further investigated the structural properties of the internal lipid molecules. We found that the lipid molecules on the left side of the indentation point rotate clockwise during the indentation and counterclockwise on the right side. This behavior occurred because the lipid molecules tilt to the left side in this study; therefore, the left part of the membrane suffers mainly a shearing strain in the course of indentation, whereas the right part suffers a bending strain. Moreover, the local nematic order parameter in the central regions of the membrane exhibits a valleylike pattern in the purely bending stage. It indicates the occurrence of an internal structural transition. This transition was further confirmed by calculating two kinds of included angles between neighboring lipid molecules. Lipids in the central regions transformed from a bilayered structure to an interdigitated gel structure. The transition progressively propagates to the neighboring regions. Consequently, the purely bending stage is divided into three phases: a bilayer, a transient, and an interdigitated layer. The study of the CM distance between neighboring lipid molecules showed that the lipid molecules separate from each other under indentation. By separating the distance into the normal

distance and the shear displacement, we found that the normal distance determines the occurrence of the transition. An interdigitated phase is formed when the normal distance becomes large enough to allow docking between the lipid molecules in the upper and lower leaflets of the bilayered membrane. Finally, the force−indentation curve has been studied. The results showed two linear regimes. In the first regime, the lipid membrane behaves elastically. The apparent spring constant calculated from the line slope shows consistency with experiments. In the second regime, the internal phase transition takes place. The extension of the membrane dimension upon indentation reduces the lateral stress, hence the apparent spring constant is small. Unlike metal or ceramic, lipid membranes are flexible, soft, and diffusible. These characteristics give them the possibility to adapt themselves against external actions through structural transformation or reassembly. The study performed here opens a window for the details of lipid membranes under indentation on the molecular level and provides valuable information in understanding the stability of pore-spanning lipid membranes.

In perspective, there are several topics to be investigated. For example, a true 3D model that includes the correct hydrodynamic effect should be used in the future to clarify some points in our quasi-2D model. How will the structural transition of the membrane be formed under a probe indentation with respect to the tilting direction of lipid molecules? Will the strain be propagated outward from the indenting center, with respect to some kind of geometrical symmetry (e.g., ellipsoidal)? How do the hydrophobic or hydrophilic characteristics of probes and pore substrates affect the response of the membrane? What role does the tilting of lipid molecules play in the indentation study? A theoretical analysis should be developed to explain the possible impact of the structural transition on the force−indentation curves.

AUTHOR INFORMATION

Corresponding Author

*E-mail: pyhsiao@ess.nthu.edu.tw.

ACKNOWLEDGMENT

This material is based upon work supported by the National Science Council and the Republic of China under contract nos. 97-2627-M-007-005, 98-2627-M-007-004, and 99-2627-M-007-004.

REFERENCES

(1) Alberts, B.; Bray, D.; Hopkin, K.; Johnson, A. *Essential Cell Biology*; Garland Science: New York, 2010.
(2) Gennis, R. B. *Biomembranes: Molecular Structure and Function*; Springer-Verlag: New York, 1989.
(3) Ellison, L.; Michel, D.; Barmes, F.; Cleaver, D. *Phys. Rev. Lett.* **2006**, *97*, 237801.
(4) Lee, W.; Mezzenga, R.; Fredrickson, G. *Phys. Rev. Lett.* **2007**, *99*, 187801.
(5) Angelov, B.; Angelova, A.; Garamus, V. M.; Lebas, G.; Lesieur, S.; Ollivon, M.; Funari, S. S.; Willumeit, R.; Couvreur, P. *J. Am. Chem. Soc.* **2007**, *129*, 13474.
(6) Lenz, O.; Schmid, F. *Phys. Rev. Lett.* **2007**, *98*, 058104.
(7) Stevens, M.; Hoh, J.; Woolf, T. *Phys. Rev. Lett.* **2003**, *91*, 188102.
(8) Grafmüller, A.; Shillcock, J.; Lipowsky, R. *Phys. Rev. Lett.* **2007**, *98*, 218101.
(9) Li, S.; Zhang, X.; Dong, W.; Wang, W. *Langmuir* **2008**, *24*, 9344.
(10) Stevens, M. J. *J. Chem. Phys.* **2004**, *121*, 11942.
(11) Lenz, O.; Schmid, F. *J. Mol. Liq.* **2005**, *117*, 147.
(12) Kranenburg, M.; Venturoli, M.; Smit, B. *J. Phys. Chem. B* **2003**, *107*, 11491.
(13) Kranenburg, M.; Vlaar, M.; Smit, B. *Biophys. J.* **2004**, *87*, 1596.
(14) Furuike, S.; Levadny, V. G.; Li, S. J.; Yamazaki, M. *Biophys. J.* **1999**, *77*, 2015.
(15) Koynova, R.; Caffrey, M. *Biochim. Biophys. Acta, Rev. Biomembr.* **1998**, *1376*, 91.
(16) Venturoli, M.; Maddalenasperotto, M.; Kranenburg, M.; Smit, B. *Phys. Rep.* **2006**, *437*, 1.
(17) Stora, T.; Dienes, Z.; Vogel, H.; Duschl, C. *Langmuir* **2000**, *16*, 5471.
(18) Lahiri, J.; Kalal, P.; Frutos, A. G.; Jonas, S. T.; Schaeffler, R. *Langmuir* **2000**, *16*, 7805.
(19) Lin, Y.; Huang, K.; Chiang, J.; Yang, C.; Lai, T. *Sens. Actuators, B* **2006**, *117*, 464.
(20) Simon, A.; Girard-Egrot, A.; Sauter, F.; Pudda, C.; Picollet D'Hahan, N.; Blum, L.; Chatelain, F.; Fuchs, A. *J. Colloid Interface Sci.* **2007**, *308*, 337.
(21) Maurer, J. A.; White, V. E.; Dougherty, D. A.; Nadeau, J. L. *Biosens. Bioelectron.* **2007**, *22*, 2577.
(22) Chang, J. M.; Tseng, F. G.; Chieng, C. C. *IEEE Trans. Nanobiosci.* **2010**, *9*, 289.
(23) Safinya, C. R.; Roux, D.; Smith, G. S.; Sinha, S. K.; Dimon, P.; Clark, N. A.; Bellocq, A. M. *Phys. Rev. Lett.* **1986**, *57*, 2718.
(24) Nagle, J. F.; Tristram-Nagle, S. *Biochim. Biophys. Acta, Rev. Biomembr.* **2000**, *1469*, 159.
(25) Salditt, T.; Li, C.; Spaar, A.; Mennicke, U. *Eur. Phys. J. E* **2002**, *7*, 105.
(26) Salditt, T. *Curr. Opin. Struct. Biol.* **2003**, *13*, 467.
(27) Miller, C. E.; Majewski, J.; Gog, T.; Kuhl, T. L. *Phys. Rev. Lett.* **2005**, *94*, 238104.
(28) Novakova, E.; Giewekemeyer, K.; Salditt, T. *Phys. Rev. E* **2006**, *74*, 051911.
(29) Sackmann, E. *Science* **1996**, *271*, 43.
(30) Beerlink, A.; Wilbrandt, P. J.; Ziegler, E.; Carbone, D.; Metzger, T. H.; Salditt, T. *Langmuir* **2008**, *24*, 4952.
(31) Hennesthal, C.; Steinem, C. *J. Am. Chem. Soc.* **2000**, *122*, 8085.
(32) McGeoch, J. E. M.; McGeoch, M. W.; Carter, D. J. D.; Shuman, R. F.; Guidotti, G. *Med. Biol. Eng. Comput.* **2000**, *38*, 113.
(33) Trojanowicz, M. *Fresenius' J. Anal. Chem.* **2001**, *371*, 246.
(34) Mey, I.; Stephan, M.; Schmitt, E. K.; Muller, M. M.; Ben Amar, M.; Steinem, C.; Janshoff, A. *J. Am. Chem. Soc.* **2009**, *131*, 7031.
(35) Gonçalves, R. P.; Agnus, G.; Sens, P.; Houssin, C.; Bartenlian, B.; Scheuring, S. *Nat. Methods* **2006**, *3*, 1007.
(36) Kwok, R.; Evans, E. *Biophys. J.* **1981**, *35*, 637.
(37) Evans, E.; Needham, D. *J. Phys. Chem.* **1987**, *91*, 4219.
(38) Needham, D.; McIntosh, T. J.; Evans, E. *Biochemistry* **1988**, *27*, 4668.
(39) Needham, D.; Nunn, R. S. *Biophys. J.* **1990**, *58*, 997.
(40) Rawicz, W.; Olbrich, K. C.; McIntosh, T.; Needham, D.; Evans, E. *Biophys. J.* **2000**, *79*, 328.
(41) Evans, E.; Heinrich, V.; Ludwig, F.; Rawicz, W. *Biophys. J.* **2003**, *85*, 2342.
(42) Tieleman, D. P.; Leontiadou, H.; Mark, A. E.; Marrink, S. J. *J. Am. Chem. Soc.* **2003**, *125*, 6382.
(43) Leontiadou, H.; Mark, A. E.; Marrink, S. J. *Biophys. J.* **2004**, *86*, 2156.
(44) Neder, J. r.; West, B.; Nielaba, P.; Schmid, F. *J. Chem. Phys.* **2010**, *132*, 115101.
(45) Steltenkamp, S.; Müller, M. M.; Deserno, M.; Hennesthal, C.; Steinem, C.; Janshoff, A. *Biophys. J.* **2006**, *91*, 217.
(46) Fine, T.; Mey, I.; Rommel, C.; Wegener, J.; Steinem, C.; Janshoff, A. *Soft Matter* **2009**, *5*, 3262.
(47) Chandross, M.; Lorenz, C. D.; Stevens, M. J.; Grest, G. S. *Langmuir* **2008**, *24*, 1240.
(48) Chandross, M.; Lorenz, C. D.; Stevens, M. J.; Grest, G. S. *ASME J. Manuf. Sci. Eng.* **2010**, *132*, 030916.

(49) Wallace, E. J.; Sansom, M. S. P. *Nano Lett.* **2008**, *8*, 2751.
(50) Shelley, J. C.; Shelley, M. Y.; Reeder, R. C.; Bandyopadhyay, S.; Moore, P. B.; Klein, M. L. *J. Phys. Chem. B* **2001**, *105*, 9785.
(51) Bennun, S. V.; Dickey, A. N.; Xing, C.; Faller, R. *Fluid Phase Equilib.* **2007**, *261*, 18.
(52) Español, P.; Warren, P. B. *Europhys. Lett.* **1995**, *30*, 191.
(53) Groot, R. D.; Warren, P. B. *J. Chem. Phys.* **1997**, *107*, 4423.
(54) Malevanets, A.; Kapral, R. *J. Chem. Phys.* **2000**, *112*, 7260.
(55) Gompper, G.; Ihle, T.; Kroll, D.; Winkler, R. In *Advanced Computer Simulation Approaches for Soft Matter Sciences III*; Holm, C., Kremer, K., Eds.; Springer: Berlin, 2009; Vol. 221, p 1.
(56) Ovalle-García, E.; Torres-Heredia, J. J.; Antillón, A.; Ortega-Blake, I. *J. Phys. Chem. B* **2011**, *115*, 4826.
(57) Helm, C.; Israelachvili, J.; McGuiggan, P. *Science* **1989**, *246*, 919.
(58) Nose, S. *Mol. Phys.* **1984**, *52*, 255.
(59) Nose, S. *J. Chem. Phys.* **1984**, *81*, 511.
(60) The simulations were run using the LAMMPS package (http://lammps.sandia.gov/).
(61) The word "indentation" might give people an impression that a small toothlike notch is made on the surface of the membrane. However, the truth is that a nonsupported membrane allows a large sink deformation of several times the membrane thickness by a probe indentation, and the membrane dimension is largely elongated before rupture occurs. However, people commonly describe the phenomenon as "indentation by a probe" instead of "elongation by a probe" in the literature (refs 34, 35, 45, 56, and 70). Therefore, we use the word "indentation" in this article.
(62) Martyna, G. J.; Tobias, D. J.; Klein, M. L. *J. Chem. Phys.* **1994**, *101*, 4177.
(63) de Gennes, P. G.; Prost, J. *The Physics of Liquid Crystals*; Clarendon Press: Oxford, U.K., 1993.
(64) Matsuki, H.; Okuno, H.; Sakano, F.; Kusube, M.; Kaneshina, S. *Biochim. Biophys. Acta, Biomembr.* **2005**, *1712*, 92.
(65) Nagle, J. F.; Zhang, R. T.; TristramNagle, S.; Sun, W. J.; Petrache, H. I.; Suter, R. M. *Biophys. J.* **1996**, *70*, 1419.
(66) Tristramnagle, S.; Zhang, R.; Suter, R. M.; Worthington, C. R.; Sun, W. J.; Nagle, J. F. *Biophys. J.* **1993**, *64*, 1097.
(67) Tenchov, B.; Koynova, R.; Rapp, G. *Biophys. J.* **2001**, *80*, 1873.
(68) McIntosh, T. J. *Biophys. J.* **1980**, *29*, 237.
(69) Kocun, M.; Mueller, W.; Maskos, M.; Mey, I.; Geil, B.; Steinem, C.; Janshoff, A. *Soft Matter* **2010**, *6*, 2508.
(70) Norouzi, D.; Muller, M. M.; Deserno, M. *Phys. Rev. E* **2006**, *74*, 061914.